# Influence of material model and modeling space on the precision of a finite element simulation to predict the deformation of silicone rubber

# Influencia del modelo del material y espacio de modelado en la precisión de una simulación con elementos finitos para predecir la deformación en silicona

**Elizabeth Mesa-Múnera[1], M. Sc., Juan F. Ramírez-Salazar[1], & M. Sc., Walter F. Bischof, Ph. D[2], Pierre Boulanger[2], Ph. D. & John W. Branch[1], Ph. D.**
1. Escual de Ingenieria de Sistemas, Facultad de Minas, Universidad Nacional de Colombia
2. Department of Computing Science, University of Alberta, Canada
*emesamun@unal.edu.co, jframiresa@unal.edu.co, wfb@ualberta.ca, pierreb@ualberta.ca, jwbranch@unal.edu.co*

Recibido para revisión 18 de junio de 2011, aceptado 18 de octubre de 2011, versión final 24 de noviembre de 2011

***Abstract*** **— The realistic simulation of tool-tissue interactions is required for the development of surgical simulators. In this paper, we estimate the material properties of a silicone rubber with mechanical properties similar to brain tissue, by performing a standard compression test. Using the estimated parameters, we performed different finite element simulations of needle indentation into a block of the same tissue. We investigated the effect of material model (Neo-Hookean and Second Order Reduced Polynomial) and modeling space (3D and axisymmetric geometries) on the accuracy of the simulation. We demonstrated that material model, space and their interaction have a significant effect on the accuracy of the simulations. The most accurate combination corresponds to a 3D simulation using a Reduced Polynomial model. However, even for not-axisymmetric geometries, one can sacrifice some accuracy and use a simpler and faster modeling space (i.e. axisymmetric), at least for the simulations considered here, given a change in the modeling space has a smaller effect on accuracy than a change in the material model.**

***Keywords*** **— Soft tissue characterization, brain indentation, Finite Element Method, Design of Experiments.**

***Resumen*** **— Una auténtica simulación de interacciones tejido-herramienta es un requerimiento para el desarrollo de simuladores quirúrgicos. En este artículo fueron estimadas las propiedades de una silicona que tiene un comportamiento similar al tejido cerebral por medio de una prueba de compresión estándar. Posteriormente, utilizando los parámetros estimados con anterioridad, se desarrollaron diferentes simulaciones de indentación de agujas en un bloque del mismo material, utilizando el Método de Elementos Finitos. Se desarrolló un diseño experimental con el fin de investigar el efecto del modelo del material (Neo-Hookeano y Polinomial reducido de segundo orden) y del espacio de modelación (geometrías tridimensionales y axisimétricas) en la precisión de la simulación. Se demostró que el tipo de modelo del material, el espacio de estudio y su respectiva interacción, tienen un efecto significativo en la precisión de la simulación. La combinación de factores que produjo el mejor resultado corresponde a la mezcla de un modelo 3D y un modelo polinomial reducido. No obstante, aun para simulaciones de este tipo donde no se utilicen modelos axisimétricos, se puede aproximar la solución con modelos más sencillos y eficientes (es decir, axisimétricos) teniendo en cuenta que el efecto de cambiar el modelo geométrico no tiene un impacto tan notorio como el cambio en el tipo de material.**

***Palabras Clave*** **— Caracterización de tejidos blandos, Indentación en el cerebro, Método de elementos finitos, Diseño de experimentos.**

## I. INTRODUCTION

Surgical simulation has revolutionized the way novice surgeons are being trained. Current training of surgeons works with real-life cases, phantom samples and animal specimens or cadavers, leading difficulties with ethics approval and the ability to evaluate performance. The realistic simulation of surgical procedures is considered an effective and safe method for the development of surgical training and planning, by emphasizing real-time interaction with medical instruments and realistic virtual models of patients. Surgical simulators have been developed for a wide range of procedures and they can be classified into three main categories, needle-based, minimally invasive, and open surgery. Needle insertion is a well-known procedure due to its application in Minimally Invasive Surgeries (MIS), such as biopsies, brachytherapy, neurosurgery, and tumor ablation. Neurosurgical needle insertion is a type of MIS that is performed with a restricted field of view, displaced 2D

Revista Avances en Sistemas e Informática, Vol.8 No. 3, diciembre de 2011 - Medellín. ISSN 1657-7663

visual feedback, and distorted haptic feedback. Much research and development has been devoted for training surgeons in MIS using visual and haptic feedback, but the accurate characterization of soft tissues for haptic simulation remains an open research area [1].

Haptic models, which include relationships between forces and displacements during the simulated medical procedure, are usually based on biomechanical models. To simulate realistic surgical interventions for needle insertion into the brain, it is necessary to implement algorithms that are accurate and are computationally efficient [2]. Furthermore, the accuracy of planning in medical interventions and the credibility of surgical simulation depend on soft-tissue constitutive laws, the shape of the surgical tool, organ geometry and boundary conditions imposed by the connective tissues surrounding the organ. Considering the current development of real-time deformable models for surgery simulation, the techniques to acquire brain properties and the integration of haptic feedback into surgical training interfaces, it is still necessary to implement experimental studies to measure mechanical properties of soft tissue and compare the results obtained with tool-tissue interaction models with empirical data. Some researchers have evaluated soft tissue properties in-vivo, ex-vivo, or in phantom tissues, using stretch tests [3], aspiration experiments [4], compression tests and, needle insertion, for linear [5] and non-linear bio-mechanical models [6]. In all these cases, researchers showed that their parameters correctly fit the experimental data used in a material calibration. However, they did not evaluate the estimated material properties in different types of experimental setups by comparing the results with additional experimental data. It is for this reason that we estimate the material properties of a silicone rubber cube with similar mechanical properties as brain matter by performing a standard compression test. In addition, we validate the results of the estimated parameters by simulating a needle indentation and comparing the results with the corresponding experimental data. In our study, we also evaluate the effect of modeling space and material models on the accuracy of the Finite Element Method (FEM) to simulate needle indentation in soft tissue. Our results can be applied to a variety of medical applications, but we focus on brain biopsies in which physicians use a needle. The obtained material model can be used for subsequent surgical simulations that include haptic feedback during the indentation of a needle into a virtual brain. Results showed that the Neo-Hookean material model fits the experimental compression test data with a R-squared error of  while the error with Reduced Polynomial Model was . Based on the results of the experimental design, we conclude that the effect of changing material model is more significant than the effect of changing the modeling space. Related work and theoretical foundations on tissue characterization and needle insertion simulation is reviewed in Section 2. In Section 4 we describe the methods and experiments to calibrate the material and to simulate needle indentation into soft tissue, followed by the results of each approach. Finally in Sections 5 and 6, we present the discussion and conclusions of our study.

## II. RELATED WORK

This section presents previous work in soft tissue characterization using different measurement techniques and different numerical approximations. In addition, we discuss studies on indentation and needle insertion into soft tissue.

### A. Soft-tissue Characterization

To produce a realistic approximation of soft tissue in virtual environments for surgical simulation, it is important to develop accurate mathematical models that predict the behavior of soft tissue. Tissue characterization, also called calibration, consists on the definition of material properties based on the measurement of tool-tissue interaction forces and deformations. The measurements can be done using several invasive and non-invasive techniques and devices to obtain material properties of animals, human and phantom specimens. Previous work on soft tissue characterization can be classified in several ways. Some researchers use indentation techniques [5][6][7], others consider stretching [3], aspiration [4], compression [8], among many other techniques. Additionally, results have been reported on different organs from animals and human samples, such as liver [9], brain [10][11] and kidney [6]. Considering the limitations and advantages of the measurement techniques, some researchers have used *ex-vivo* experiments and phantom tissues, as they allow precise control of the sample and experimental conditions for modeling [5][7][12]. Finally, due to the many factors involved in soft tissue deformation, there are numerous constitutive biomechanical models that can be used to simulate different material behaviors. Some materials can be successfully defined by very simple approximations based on Hooke's Law, as shown by DiMaio and Salcudean in [5]. However, more complex materials, such as liver, kidney and brain, require the use of viscoelastic and hyperelastic constitutive models. Kim et al. [6] determined the hyper-viscoelastic properties of intra-abdominal organs in-vivo using an indentation device. They implemented a tridimensional inverse Finite Element (FE) parameter estimation algorithm and they assumed the quasi-linear-viscoelastic theory proposed by Fung [13]. As mentioned earlier, previous work on tissue calibration obtained material properties based on experimental data, but researchers usually did not evaluate and validate model performance in different applications. This is a crucial evaluation. For instance, Miller et al. [10] demonstrated that swine brain tissue is considerably softer in extension than in compression. Therefore, these parameters should be carefully selected according to the application that needs to be simulated.

### B. Simulation of Needle Insertion and Indentation

Different deformable models have been used for interactive object simulation. These models can be selected according to the application where parameters such accuracy or speed may be not relevant. In surgical training, the main requirement is accuracy and the use of pre-recorded data is feasible. However,

deformable models for surgical simulation need to be fast but, at the same time, keeping an acceptable level of fidelity to allow real-time interactivity. According to Abolhassani et al. [1], the simulation of needle insertion into soft tissue can be divided in pre-puncture, or indentation, and post-puncture phases. DiMaio [5] simulated needle insertion using a linear elastic material model and 2D and 3D FEM. He emphasized the importance of 3D models for this type of simulation and the necessity of having accurate 3D measurements in tissue phantoms [14]. Okamura et al. [9] modeled the forces during needle insertion into bovine liver using a second order polynomial material model and non-linear spring system. They also evaluated the effect of needle diameter on the insertion force using a silicone rubber phantom. They concluded that smaller needle diameters lead to less resistance force but more needle bending. Horton et al. [15][16] implemented a meshless method to model the indentation of brain tissue using moving least squares shape functions and a Neo-Hookean material model. Many other authors have worked on the simulation of needle indentation into soft tissue using FEM, for example [6][7][16][17].

## III. THEORETICAL FOUNDATION

Different constitutive laws are used to model the mechanical response of a material according to its behavior [18]. These models are obtained by fitting experimental measurements to a set of equations that relate stresses and strains. Even if the constitutive models are not acquired using fundamental physical laws, they must satisfy the laws of thermodynamics. In the present study, we used the Hyperelasticity framework to model the behavior of silicone rubber

### A. Hyperelasticity

These constitutive laws apply for materials that show an elastic behavior under very large strains. Hyperelastic models are required when the material is subjected to finite displacements, whereas elastic theory is restricted to infinitesimal displacements. Hyperelasticity constitutes the basis for more complex material models, including phenomena such as viscoelasticity and tissue damage.

Suppose that the position of a particle in the material is originally located at $x_i = (x_1, x_2, x_3)$ and is then moved to a location $y_i = (y_1, y_2, y_3)$ in the deformed body. The displacement vector ($u_i$) is defined by $u_i(x_1, x_2, x_3, t) = y_i - x_i$ and the deformation gradient tensor ($F_{ij}$) corresponds to $F_{ik} = \delta_{ik} + \partial u_i / \partial x_k$, where $\delta_{ik}$ is the Kronecker delta. The constitutive equation for a hyperelastic material is derived from an analytic function of the strain energy density ($W$) with respect to $F_{ij}$. The strain energy can be defined in terms of the invariants ($I_1, I_2, I_3$) of the Left Cauchy Green Deformation Tensor (*B*), the alternative invariants ($\bar{I}_1, \bar{I}_2, J$) of *B*, or in terms of the principal stretches ($\lambda_1, \lambda_2, \lambda_3$), as shown by Eq.1.

$$W(F_{ij}) = U(I_1, I_2, I_3) = \bar{U}(\bar{I}_1, \bar{I}_2, J) = \tilde{U}(\lambda_1, \lambda_2, \lambda_3), \quad (1)$$

where $J = \det(F)$ is the Jacobian of the deformation gradient tensor. Later, $W$ is related to the Cauchy Stress Tensor ($\sigma_{ij}$) to model the behavior of a hyperelastic material (see Eq.2).

$$\sigma_{ij} = \frac{1}{J} F_{ik} \frac{\partial W}{\partial F_{kj}}. \quad (2)$$

Depending on the complexity of the Strain Energy Function $(W)$, different features such as nonlinearity and anisotropy can be included into the model. Some of the most representative forms of the Strain Energy density, usually included in commercial FEM software [19] and considered in this study, are described as follows:

Reduced Polynomial
$$\bar{U} = \sum_{i=1}^{N} C_{i0} (\bar{I}_1 - 3)^i + \sum_{i=1}^{N} \frac{K_i}{2} (J-1)^{2i}, \quad (3)$$

Neo-Hookean Solid
$$\bar{U} = C_{10} (\bar{I}_1 - 3) + \frac{K_1}{2} (J-1)^2,$$

where $C_{i0}$, $K_i$ are temperature-dependent material parameters and are related to the initial shear modulus ($\mu$) and the bulk modulus ($K$) by Eq. 4.

$$\mu = 2\, C_{10}, \qquad K = K_1. \quad (4)$$

Soft biological tissues can be approximated as nearly incompressible materials based on their high water content. To model this approximation using the previous models, one simply sets the last term to zero. This is because the Jacobian ( $J$) of the deformation gradient is equal to 1 in the case of fully incompressible materials; hence the second term is null.

### B. Analytical solution of a Compression test

In the compression test, the material is submitted only to a normal stresses because the contact surfaces between the plates and the material are lubricated. Let us also assume an incompressible, homogeneous, isotropic material; therefore the transverse strains $\epsilon_2$ and $\epsilon_3$ (perpendicular to the applied load) are considered to be the same. Using the definition of the Poisson's ratio ($\nu$), we can relate the transverse strains with the axial strain $\epsilon_1$ (in the same direction of the load) using the relation presented in Eq. 5 [20].

Revista Avances en Sistemas e Informática, Vol.8 No. 3, diciembre de 2011 - Medellín. ISSN 1657-7663

$$\lambda_2 = \lambda_3 = \lambda_1^{-\nu}, \quad (5)$$

where $\lambda_i = 1 + \epsilon_i$. Using the definitions in Eq.2 and Eq.3, the Cauchy Stress Tensor for the incompressible Neo-Hookean solid is given by Eq. 6.

Neo-Hookean Solid

$$\sigma_{ij} = 2C_{10}\left(B_{ij} - \frac{1}{3}B_{kk}\delta_{ij}\right), \quad (6)$$

where $B_{ij}$ is the Left Cauchy-Green deformation tensor and is defined as $B_{ij} = F_{ik}F_{jk}$. For an uniaxial test, the deformation gradient is a diagonal matrix with components $\lambda_1$, $\lambda_2$ and $\lambda_3$, respectively. Hence, $\sigma_{ij}$ is zero when $i \neq j$ and $\sigma_{11}$ is given by Eq. 7.

$$\sigma_{11} = 2C_{10}(\lambda_1^2 - \lambda_1^{-1}), \quad (7)$$

assuming $\nu = 0.5$ for an incompressible material. While the Cauchy Stress Tensor depends on the *deformed* solid information, the Nominal Stress Tensor ($S_{ij}$) corresponds to the internal force per unit of *undeformed* area acting within a solid, and it is the one that should be considered in the material calibration. The analytical solution of the standard compression test in terms of $S_{ij}$ is given by Eq.8.

$$S_{11} = 2C_{10}(\lambda_1 - \lambda_1^{-2}). \quad (8)$$

The analytical solution for the Second Order Reduced Polynomial model can be obtained similarly (see Eq.9).

$$S_{11} = 2(\lambda_1 - \lambda_1^{-2})(C_{10} + 2C_{20}\{(\lambda_1^2 + 2\lambda_1^{-1}) - 3\}). \quad (9)$$

## IV. MATERIAL PROPERTIY ESTIMATION AND EXPERIMENTAL METHODS

### A. Estimation of Silicone Rubber Properties

As shown by Francheschini et al. [21], human brain tissue deforms similar to filled elastomers, and it should be modelled as a nonlinear solid with small volumetric compressibility. Girnary [22] also highlight that silicone brain phantoms provide good results to simulate brain behavior. In the present study, we determined the parameters for the Neo-Hookean and Reduced Polynomial hyperelastic models to simulate the mechanical behavior of a platinum-cure silicone rubber (Ecoflex 00-10, from Smooth-On, Inc.) submitted to a compression test. We used a tissue phantom rather than biological tissue because this facilitates obtaining repeatable results in a controlled environment. Each component of the rubber solution was evenly mixed according to the recommendations of the manufacturer and then formed in a cylindrical mold of $38\ mm$ diameter and $9mm$ height. We used a force/torque sensor, (ATI Mini40 SI-40-2) with 0.02 N resolution, attached to a laparoscopic grasping tool, which was fixed to a rigid plate (see Fig. 1). The plate was displaced using a stepper motor to compress the tissue at a constant velocity of 0.4 mm/s, until the plate was displaced by 2 mm. The contact areas were lubricated with talcum powder in order to minimize lateral friction.

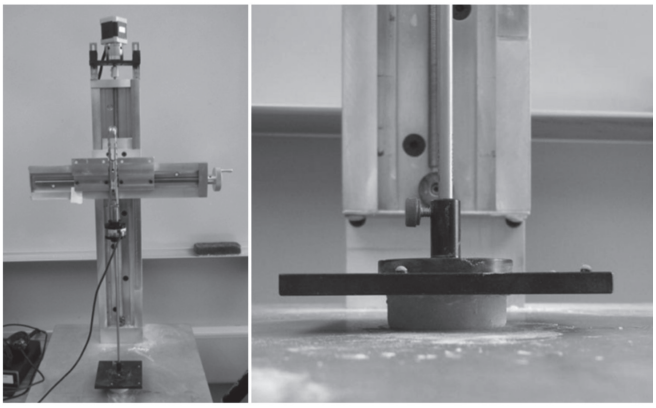

**Figure 1.** Experimental setup for the compression test of a cylindrical shape of silicon rubber (Ecoflex -0010). The surfaces were lubricated and the tissue was compressed to a strain of 0.227

Calibration of soft tissue consists of determining the material constants by minimizing the difference between the analytical solution (for simple approaches) with respect to experimental measurements through a least-squares-fit procedure using the Quasi-Newton Method (see Eq. 10). In this study, the calibration of the material models, presented by Eq.3, was done using the corresponding analytical solution of the standard compression test, as defined in Eqs.8 and 9. We used absolute errors, instead of relative errors, because this gives a better fit for large strains.

$$\min\{absolute\ error^2\} = \min\left\{\sum_i^m \left(S_{experiment} - S_{analytical}\right)^2\right\}, \quad (9)$$

where *m* is the total number of data points. The experimental Nominal Stress Tensor was found by dividing the reaction force at every sample point by the undeformed contact area. The Nominal Strain corresponded to the displacement of the plate divided by the undeformed height of the cylinder. Once we obtained the material parameters, we used the "evaluate" function of ABAQUS [19] to run the Drucker stability check of the material.

### *Finite Element Modeling and Experimental Design*

The main goal of this stage was to compare different simulations of needle indentation with experimental data in order to study the influence of the material model and modeling space on the accuracy of the FEM solution. For the measurement of forces and displacement during soft tissue indentation, we used the same silicone rubber, force and torque sensors, stepper motor, and the needle was inserted at the same movement velocity. However, the specimen was a block of $70 \times 80 \times 80\ mm$, and it was indented until the deformation was $10\ mm$ (see Fig. 2). The needle had a conical shape with a rounded tip of $5mm$ diameter. We used a $2^k$ *Factorial Design,* which allowed us to find the effects of the factors and the interaction between factors [23]. The response variable was the R-Squared error between the simulation and experimental data, the factors were the material model (with levels Neo-Hookean and Reduced Polynomial) and the modeling space (with levels axisymmetric and 3D). Finally we performed two experiments to measure the reaction forces during the indentation, with the purpose of having a replicate of the experiment.

To run the simulation using the properties previously determined, we simulated an indentation in ABAQUS as contact between a rigid needle and an isotropic silicone rubber. The tangential behavior of the contact was defined using a $0.8$ friction coefficient. For the case of 3D modelling space, we generated a cube with the same characteristics of the real specimen; for the axisymmetric case, the model corresponded to a cylinder of $70\ mm$ diameter and $80mm$ height. Although this changes the approach to the problem, we will show that axisymmetric models (which are simpler than the 3D approximation) can be used to approximate problems that are not axisymmetric. In both cases, we used elements with hybrid formulation and reduced integration. The mesh size was graded to be more refined close to the indenter and coarse near the model boundaries (see Fig. 3). In all simulations, we allowed nonlinearities for the material model and for large geometric deformation. In the 3D approximation, the model was assumed to be symmetric, hence only one quarter of the cube needed to be simulated. The bottom of the deformable body was fixed in space, and both, the rigid indenter and the axis of symmetry (or planes of symmetry, in the 3D case) in the deformable object, were allowed to move only in the vertical direction. We constrained the indenter tip to the node at the upper left corner of the mesh, and we moved the indenter such that the displacement amplitude changed at a rate of $0.4mm/s0.4mm/s$ until it reached $10\ mm\ 10\ mm$.

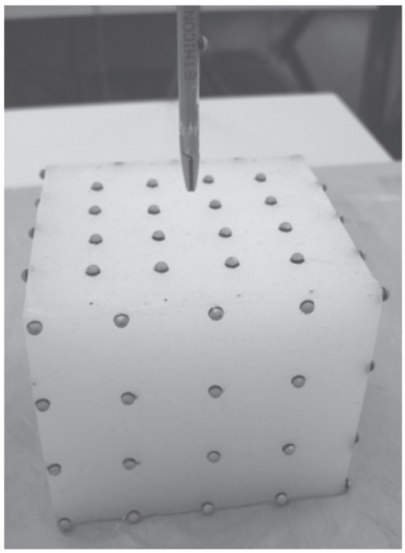

**Figure 2.** Setup for Needle Indentation in a block of 70x80x80 mm. We ensure that velocity was constant and the needle was indented until the strain corresponded to 0.14

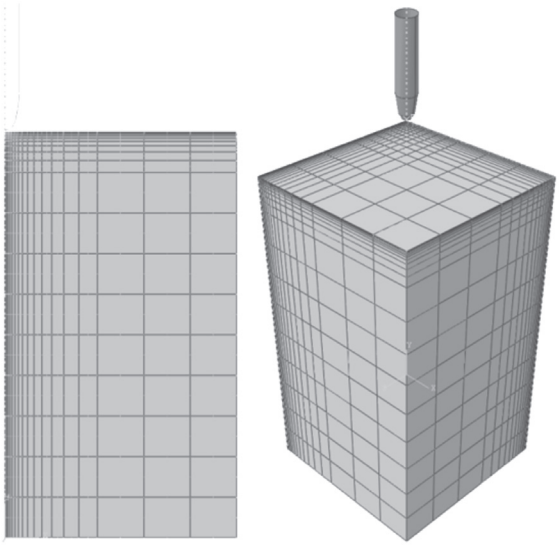

**Figure 3.** Mesh for the axisymmetric (left) and 3D models (right). The mesh was refined in the regions close to the area of contact with the indenter.

Revista Avances en Sistemas e Informática, Vol.8 No. 3, diciembre de 2011 - Medellín. ISSN 1657-7663

## V. RESULTS

This section reports the material properties that we found for the silicone rubber using the compression test data and two different material models. We also present the results of the FEM simulation of needle indentation and the comparison with the experimental measurements. We conclude this section with the results of the experimental design.

### A. Material Calibration

The stress-strain curves for the uniaxial compression test and the predicted curves using the two hyperelastic models are shown in Fig. 4. We found $C_{10} = 1101.295$ for the Neo-Hookean material model, and $C_{10} = 686.428$; $C_{20} = 1929.606$ for the second order Reduced Polynomial Model. The Drucker Stability Check showed that both models were stable for all strains. The R-squared error for the fitting given by the Neo-Hookean model was $0.8965$ and the error for the Reduced Polynomial model was $0.9648$.

### B. Simulation of Needle indentation and Experimental Design

Before we ran the experiments, we refined the mesh until the error of the simulation with respect to the experimental data did not change significantly. For the following experimental runs, we kept the same mesh parameters. The experimental matrix, which presents the different simulations that were run in this study and the resulting errors, is shown in Table 1. There were two replications of each simulation, and the table shows the R-Squared errors of the simulations with respect to the two experimental measurements.

**Table 1.** Experimental Matrix

| Material Model (Factor A) | Modeling Space (Factor B) | | | |
|---|---|---|---|---|
| | Axisymmetric (Level 1) | | 3D (Level 2) | |
| Neo-Hookean (Level 1) | 0.98024 | 0.97516 | 0.98931 | 0.98562 |
| Reduced Polynomial (Level 2) | 0.99960 | 0.99829 | 0.99976 | 0.99919 |

The results of all the FEM simulations and the experimental measurements are shown in Fig. 5. In this figure we related the reaction force in the indenter with the needle displacement. The simulations differ by the parameters of the experimental design, as shown in Table 1. The simulated distributions of stresses using axisymmetric and tridimensional models in ABAQUS are shown in Fig. 6 and Fig. 7.

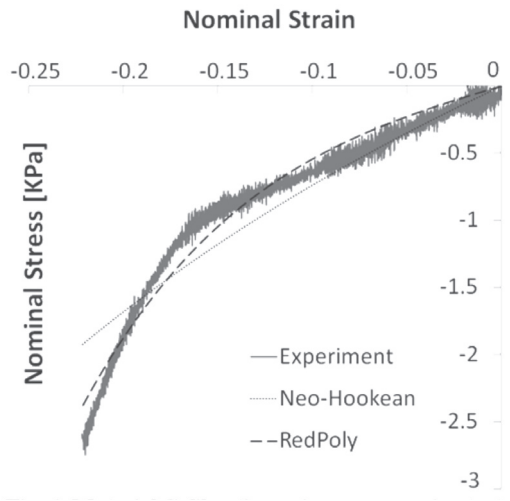


**Figure 4.** Material Calibration using compression test data

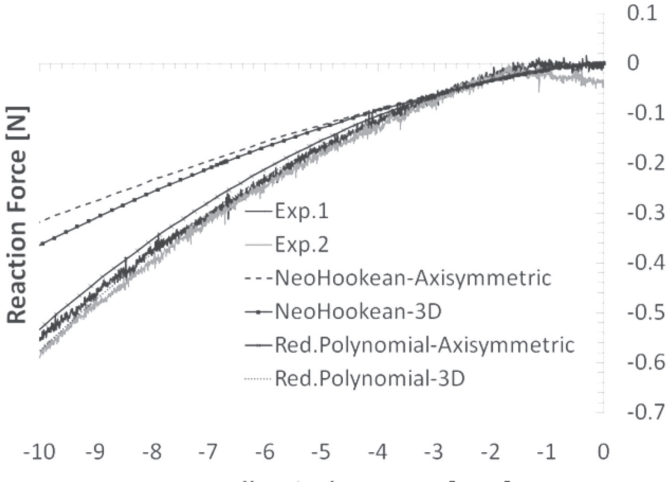


**Figure 5.** Comparison of experimental measurements with FEM simulations for a needle indentation.

An Analysis of Variance (Anova) showed that the effects of the material model, the modeling space and their interaction are statistically significant, $p = 0.001$, $p = 0.033$ and $p = 0.046 p = 0.046$, respectively. The Anova had an acceptable adjusted error of $94.57\%$, where the missing $5.43\%$ of the variability in the R-squared error of the simulation is due to the effect of factors not considered in this study. The effects sizes were $\eta^2(material) = 0.826$ $\eta^2(material) = 0.826$, $\eta^2(space) = 0.079$, and $\eta^2(material \times space) = 0.063$, indicating that the material model affect the quality of the simulation the most.

We also confirmed the adequacy of the assumptions underlying the Anova [23]. The normality test using Ryan-

Joiner Test was not significant, $p > 0.1$, indicating that the residuals were normally distributed (see Fig. 8). Furthermore, the Bartlett's Test indicated that the residual variances were homogeneous, $p = 0.409$ (see Fig. 9).

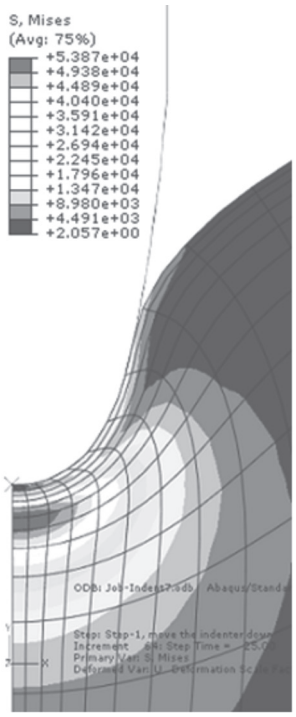


**Figure 6.** Axisymmetrical Indentation in ABAQUS

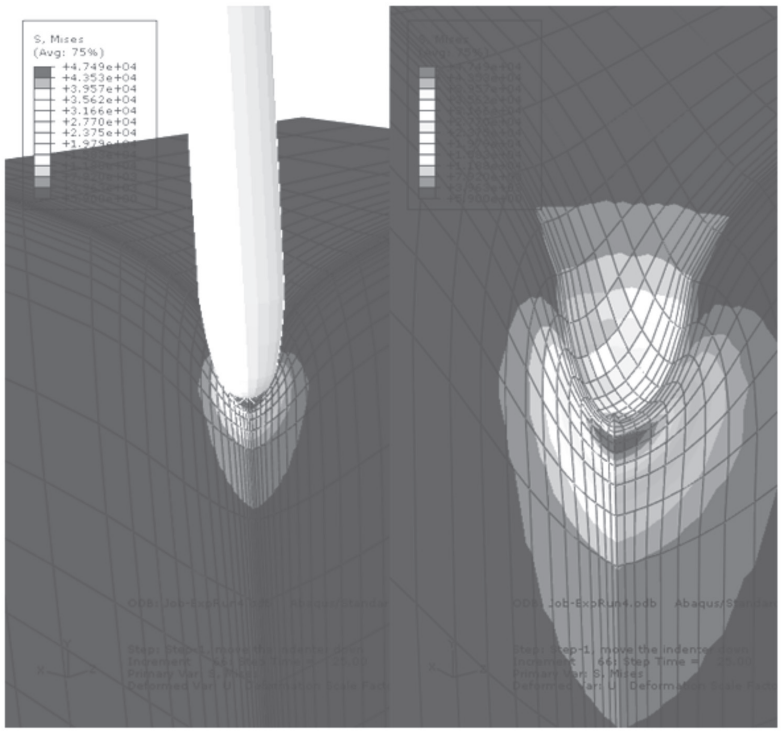

**Figure 7.** Mesh for the axisymmetric (left) and 3D models (right).

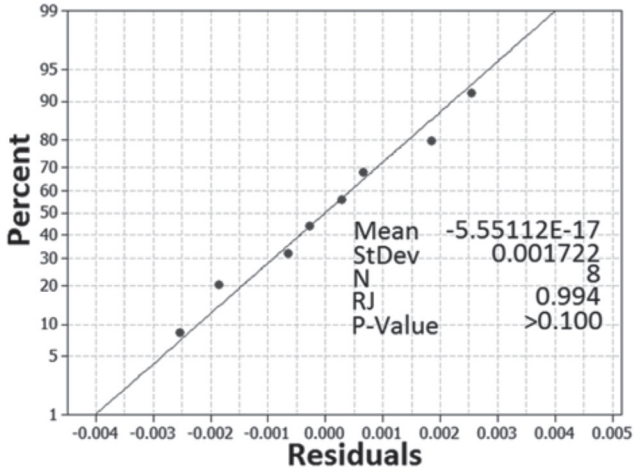


**Figure 8.** Normality Test – Ryan-Joiner

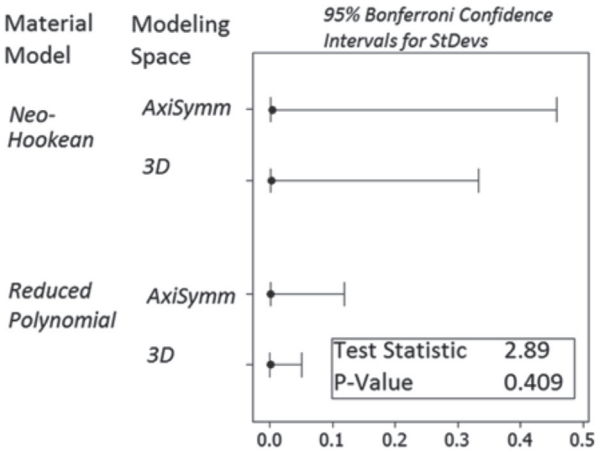


**Figure 9.** Bartlett's Test for Constant Variance

## VI. DISCUSSION AND CONCLUSIONS

In this paper, we characterized silicone rubber using the experimental measurements from a compression test. We evaluated the effect of two material models (Neo-Hookean and a Second Order Reduced Polynomial) and two modeling spaces (axisymmetric and 3D) on the R-squared error between simulated data and the experimental results of needle indentation. We concluded that, for very small velocities (in our case, for $\mathrm{v} = 0.4mm/s$), the material properties found in the compression test can be successfully used to simulate more complex interactions, e.g. needle indentation.

We also concluded that the material model, the modeling space, and the interaction between these two factors, affect the

accuracy of the simulation. However, the effect of the material model is substantially higher than the other two. Therefore, if one needs to simulate a model that is not axisymmetric, one can sacrifice some accuracy for a simpler and faster modeling space than the full 3D model. This is due to the fact that the effect of changing modeling space does not alter the simulation as much as changing material model. Fig. 5 shows that the use of a Reduced Polynomial material model with 3D and axisymmetric modeling spaces gives very similar results.

Bearing in mind that this silicone rubber has similar properties to brain matter, future work will focus on the characterization of phantom tissue under needle indentation (where the analytical solution is not easily defined) for possible applications of brain-tissue characterization during *in-vivo* experiments.

## REFERENCES

[1] Abolhassani N, Patel R, Moallem M., 2007. Needle insertion into soft tissue: A survey. In: Medical Engineering & Physics, vol. 29, pp. 413-431.

[2] Maciel A, Halic T, Lu Z, Nedel LP, De S., 2009. Using the PhysX engine for physics-based virtual surgery with force feedback. In: The International Journal of Medical Robotics and Computer Assisted Surgery, vol. 5(3), pp. 341-353.

[3] Brouwer I, Ustin J, Bentley L, Sherman A, Dhruv N, Tendick F., 2001. Measuring in vivo animal soft tissue properties for haptic modeling in surgical simulation. In: Studies in Health Technology and Informatics 69-74.

[4] Kauer M, Vuskovic V, Dual J, Szekely G, Bajka M., 2002. Inverse finite element characterization of soft tissues. In: Medical Image Analysis, vol. 6(3), pp. 275-287.

[5] DiMaio SP, Salcudean S, 2003 Needle insertion modeling and simulation. In: IEEE Transactions on Robotics and Automation, vol. 19, pp. 864-875.

[6] Kim J, Srinivasan MA, 2005 Characterization of viscoelastic soft tissue properties from in vivo animal experiments and inverse FE parameter estimation. In: Medical Image Computing and Computer-Assisted Intervention-MICCAI 2005, pp. 599-606.

[7] Nienhuys HW, van der Stappen AF, 2004 A computational technique for interactive needle insertions in 3D nonlinear material. In: ICRA'04. 2004 IEEE International Conference on Robotics and Automation, vol. 2, pp. 2061-2067.

[8] Dechwayukul C, Thongruang W., 2008. Compressive modulus of adhesive bonded rubber block. In: Songklanakarin Journal of Science and Technology, vol. 30(2), pp. 221-226.

[9] Okamura AM, Simone C, O'Leary MD, 2004 Force modeling for needle insertion into soft tissue. In: IEEE Transactions on Biomedical Engineering, vol. 51, pp. 1707-1716.

[10] Miller K, Wittek A, Joldes G, Horton A, Dutta-Roy T, Berger J, Morriss L., 2010. Modelling brain deformations for computer-integrated neurosurgery. In: International Journal for Numerical Methods in Biomedical Engineering, vol. 26(1), pp. 117-138.

[11] Kohandel M, Sivaloganathan S, Tenti G, Drake J., 2006. The constitutive properties of the brain parenchyma: Part 1. Strain energy approach. In: Medical engineering & physics, vol. 28(5), pp. 449-454.

[12] Sangpradit K, Liu H, Seneviratne LD, Althoefer K, 2009 Tissue identification using inverse Finite Element analysis of rolling indentation. In: IEEE International Conference on Robotics and Automation ICRA'09, pp. 1250-1255.

[13] Fung Y, 1993. Biomechanics: Mechanical Properties of Living Tissues. Springer.

[14] Kerdok AE, Cotin SM, Ottensmeyer MP, Galea AM, Howe RD, Dawson SL., 2003. Truth cube: Establishing physical standards for soft tissue simulation. In: Medical Image Analysis, vol. 7(3), pp. 283-291.

[15] Horton A, Wittek A, Miller K, 2007 Subject-specific biomechanical simulation of brain indentation using a meshless method. In: Medical Image Computing and Computer-Assisted Intervention-MICCAI, pp. 541-548.

[16] Miller K, Chinzei K, Orssengo G, Bednarz P., 2000. Mechanical properties of brain tissue in-vivo: experiment and computer simulation. In: Journal of Biomechanics, vol. 33(11), pp. 1369-1376.

[17] Lin DC, Shreiber DI, Dimitriadis EK, Horkay F., 2009. Spherical indentation of soft matter beyond the Hertzian regime: numerical and experimental validation of hyperelastic models. In: Biomechanics and modeling in mechanobiology, vol. 8(5), pp. 345-358.

[18] Bower AF, 2010. Applied mechanics of solids. CRC press.

[19] Simulia, Dassault Systemes. ABAQUS Analysis User s Manual, Version 6.9. [Internet]. 2005 [cited 2011].

[20] Fung Y, 1965. Foundations of Solid Mechanics. Prentice Hall.

[21] Franceschini G, Bigoni D, Regitnig P, Holzapfel GA., 2006. Brain tissue deforms similarly to filled elastomers and follows consolidation theory. In: Journal of the Mechanics and Physics of Solids, vol. 54(12), pp. 2592-2620.

[22] Girnary HH., 2007. Brain Phantom Project. Master's Thesis. Cornell University.

[23] Montgomery DC, 2001. Design and analysis of experiments. 5th ed. John Wiley & Sons Inc.